JOURNAL OF SPACECRAFT AND ROCKETS
Vol. 29, No. 6, November-December 1992

Energetics of Gas-Surface Interactions in Transitional Flows at Entry Velocities

R. G. Wilmoth*
NASA Langley Research Center, Hampton, Virginia 23681
V. K. Dogra†
Vigyan Research Associates, Inc., Hampton, Virginia 23666
and
J. N. Moss‡
NASA Langley Research Center, Hampton, Virginia 23681

The direct simulation Monte Carlo (DSMC) method has been used to calculate the molecular speed and energy distributions of molecules striking a surface after traversing a shock layer in hypersonic transitional flow. The calculations were performed for a 1.6-m-diam sphere at a nominal velocity for re-entry of 7.5 km/s over an altitude range of 130–90 km. Real gas effects and chemical reactions were included in the DSMC simulations. Results are presented for these conditions and the need for gas-surface interaction experiments is discussed.

Introduction

GAS-SURFACE interactions play an important role in the understanding of orbital and entry aerodynamics and aerothermodynamics.[1,2] Under the highly rarefied flow conditions existing at orbital altitudes, the flowfield is dominated by gas-wall collisions that occur at a mean velocity corresponding to that of the orbiting vehicle. Under entry conditions, gas-gas collisions become important, and gas molecules that reach the surface of the vehicle tend to have lost some of their translational energy (see Fig. 1). This "lost" translational energy is converted into other forms (heat, internal energy, etc.) through a variety of collision mechanisms including chemical reactions, ionization, and dissociation. Since the nature of the gas-surface interaction is known to depend on the velocity and energy of the incident molecules, it is important to know the state of the gas molecules reaching the surface.

In the direct simulation Monte Carlo (DSMC) method of Bird,[3] the molecular velocity and energy distributions of the gas molecules evolve directly as part of the simulation. The details of the gas-surface interactions are generally modeled via a simple engineering model that is based on a combination of diffuse and specular reflection with other phenomenological models used to account for processes such as catalytic reactions and recombination. These models must be applied judiciously by the analyst based on experience and a limited body of relevant experimental data. Parametric studies are frequently performed simply to place bounds on the predicted quantities of interest.[4-6] The lack of experimental data generally hinders the development of more detailed gas-surface interaction models and results mainly for two reasons. First, it is extremely difficult to simulate gas-surface interactions at orbital or entry velocities in the laboratory.[7] Also, very few flight experiments have been performed that provide meaningful gas-surface interaction data. Second, it is difficult to characterize the surfaces used in such experiments with sufficient generality that the results can be applied in an engineering context. Most of the laboratory experiments have been performed for gas velocities well below orbital and entry velocities, and many of the detailed measurements that have been made have used surfaces that were either highly idealized (e.g., single crystals) or were poorly characterized (e.g., covered by unknown oxides or contaminants). Perhaps the only general observation that can be made is that low-energy (room temperature) gas molecules tend to scatter diffusely with full thermal accommodation from room temperature engineering surfaces, whereas high-energy (greater than 1 eV) gas molecules tend to show at least some degree of specular reflection with incomplete accommodation especially at grazing angles of incidence. At the same time, little has been said about just what velocity or energy ranges are really important for gas-surface interactions occurring in flight for high-speed entry flows in the transitional to near-continuum regime. Because of the tendency of gas molecules to be "slowed" due to gas-gas collisions before reaching the surface, it is impor-

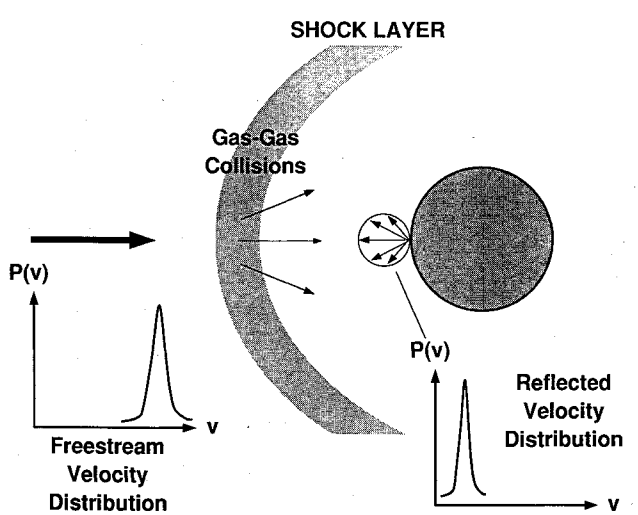

Fig. 1 Molecular velocity distributions in rarefied and transitional entry flow about a sphere.

Presented as Paper 91-1338 at the AIAA 26th Thermophysics Conference, Honolulu, HI, June 24–26, 1991; received July 2, 1991; revision received March 24, 1992; accepted for publication June 16, 1992.

*Aerospace Engineer, Aerothermodynamics Branch, Space Systems Division. Senior Member AIAA.
†Research Engineer. Member AIAA.
‡Aerospace Engineer. Aerothermodynamics Branch, Space Systems Division. Fellow AIAA.

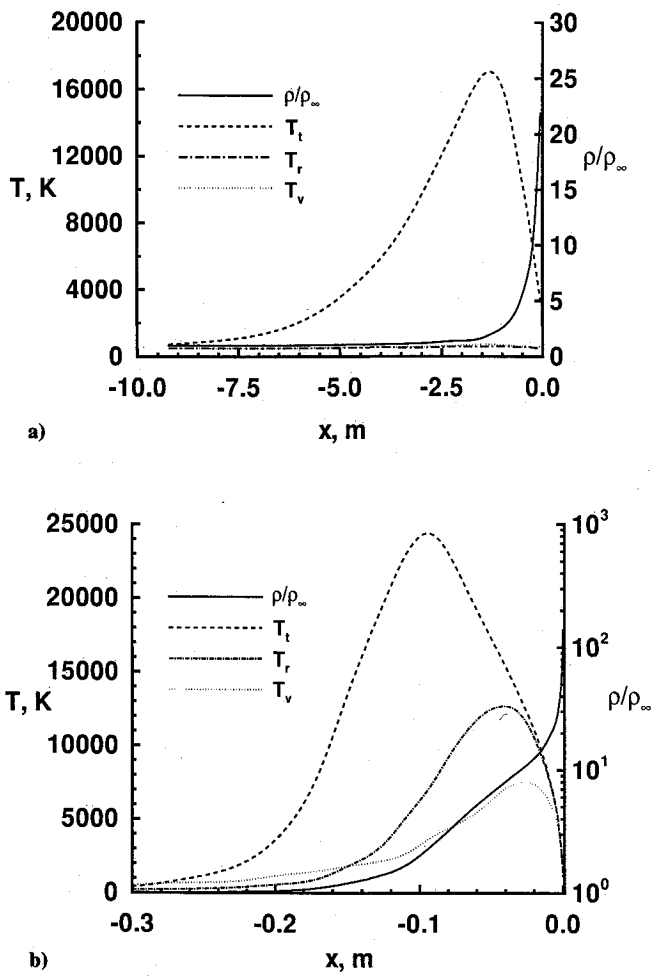

Fig. 2 Temperature and density profiles along stagnation line: a) 130 km; b) 90 km.

tant to try to quantify the velocities and energies that are actually encountered in such problems.

The purpose of this paper is to present the results of a study of the incident speeds and energies involved in gas-surface interactions for a typical transitional flow at entry velocities. The problem studied was that of a 1.6-m-diam sphere at a freestream velocity of 7.5 km/s over an altitude range of 90–130 km. This problem was selected because the basic flowfield has been well defined by previous DSMC calculations[8] and because of the implications of the results to potential experiments that may be flown on tethered satellite systems.[9,10] The previous DSMC calculations showed that this altitude range covers a wide variation in thermal and chemical nonequilibrium behavior ranging from near free-molecule flow to near-continuum flow through the shock layer (see Figs. 2 and 3).

The current study was conducted using the DSMC method of Bird[3] with the previously calculated steady-state results[8] as initial conditions. DSMC simulations were run for these conditions, and samples were taken of the speeds and translational energies of gas molecules striking the surface of the sphere. These samples were taken in such a manner that speed and energy distributions could be determined separately for each gas species and for each surface element. Because of the limited sample size, the accuracy and resolution of these distributions are not the same for all gas species and for all surface elements, e.g., the accuracy is poor for trace species and for surface elements on the leeside of the sphere. However, the sample size was sufficiently large that some meaningful insight can be obtained from the distributions for the dominant species over a significant portion of the sphere.

Method of Sampling

In the present study, attention is focused only on the magnitude of the velocity vector (speed) and translational energy of particles striking the surface without regard to direction. Therefore, the distributions to be extracted from the DSMC simulations are those which give the probability that one of these particles has a speed v (or energy e), that falls in the interval v to $v + \Delta v$ (or e to $e + \Delta e$). Such distributions are sometimes referred to as "flux" distributions because they are proportional to the product of the velocity normal to the surface with the molecular "speed" distribution of the gas, i.e., $v_n \cdot f(v)$. However, in the context of this paper, we will use the term "speed" distribution to refer to the fluxal distribution of speeds and "energy" distribution to refer to the fluxal distribution of translational energies.

In principle, the extraction of these speed and energy distributions from the DSMC simulations is straightforward. The speed and energy domains are divided into a finite number of "bins," each covering an interval from v to $v + \Delta v$ in speed and e to $e + \Delta e$ in translational energy. Each molecule striking the surface is then added to the appropriate bin according to its speed and energy. Since the error in each bin is proportional to $1/\sqrt{\text{number of samples}}$, it is desirable to have a large number of samples.

One approach to recording these samples is to accumulate the values for each individual bin (for each species and for each surface element) during the DSMC run. However, in the present study, it was decided to simply store the properties of each molecule striking the surface into a file and then postprocess the resulting data. This approach had the advantage of allowing variations in the postprocessing (such as varying the number of bins) to obtain the best overall description of the shape of the distribution with only a moderate number of samples. For the results reported herein, the total sample size

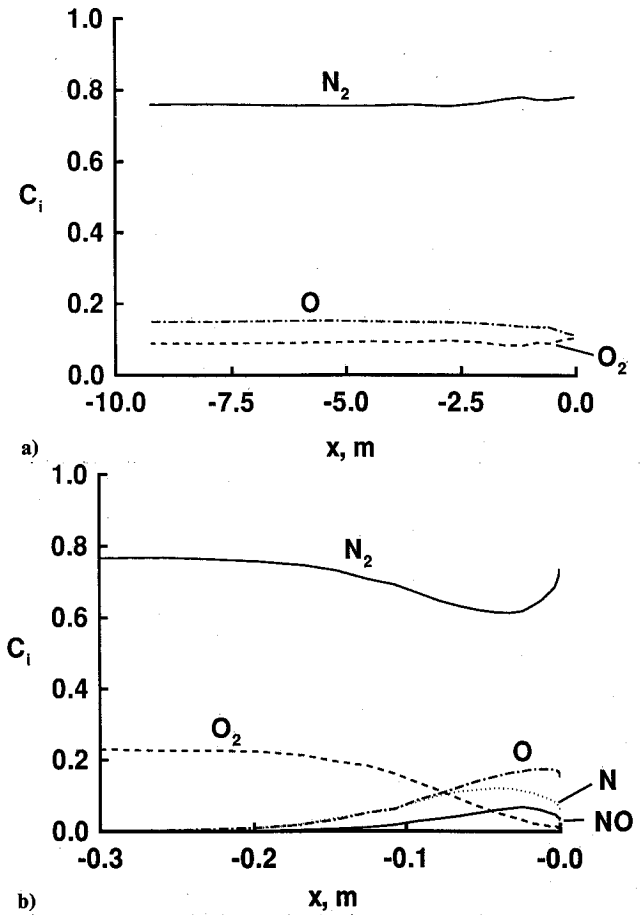

Fig. 3 Mass fractions of different species along stagnation line: a) 130 km; and b) 90 km.

(summed over all species and all surface elements) was greater than one million. A total of 25 equal-sized bins was used giving a speed resolution of about 400 m/s and an energy resolution of about 0.4 eV for each distribution. This resulted in a sample size for each species and each surface element of typically 10,000–50,000 molecules. For the dominant species (N_2, O_2, and O), the errors [i.e., in $P(v)$] due to the finite sample size are estimated to be less than 5 %, whereas for the trace species (N and NO), the errors were greater. On the leeside of the sphere, the samples were unacceptably small for all but the dominant species and for most of the surface elements. Because of the small sample sizes on the leeside, results will be presented only for conditions where the sample size is large enough to be statistically meaningful (10,000 or more particles).

Definition of Sampled Distribution Functions

The sampled distributions were normalized to give probability distribution functions as follows. Let $N_{v\to v+\Delta v}$ be the number of molecules with speeds between v and $v+\Delta v$ striking a particular surface element. (Speed is used herein to be the magnitude of the velocity vector.) A probability function, $P(v)$ is then defined by

$$P(v) = \frac{N_{v\to v+\Delta v}}{\sum_{v=0}^{\infty} N_{v\to v+\Delta v}} \tag{1}$$

which represents the fluxal distribution of speeds. Although we will refer to this as a speed distribution in this paper, it refers only to molecules striking the surface, and the reader should not confuse it with the speed distribution of all molecules in a volume element in the flowfield.

An energy probability distribution function can be defined in a manner analogous to Eq. (1) by

$$P(e) = \frac{N_{e\to e+\Delta e}}{\sum_{e=0}^{\infty} N_{e\to e+\Delta e}} \tag{2}$$

For multispecies flows, it is also convenient to define an energy probability function for species i by

$$P^i(e) = \frac{N^i_{e\to e+\Delta e}}{\sum_{i=1}^{N_{\text{species}}} \sum_{e=0}^{\infty} N^i_{e\to e+\Delta e}} \tag{3}$$

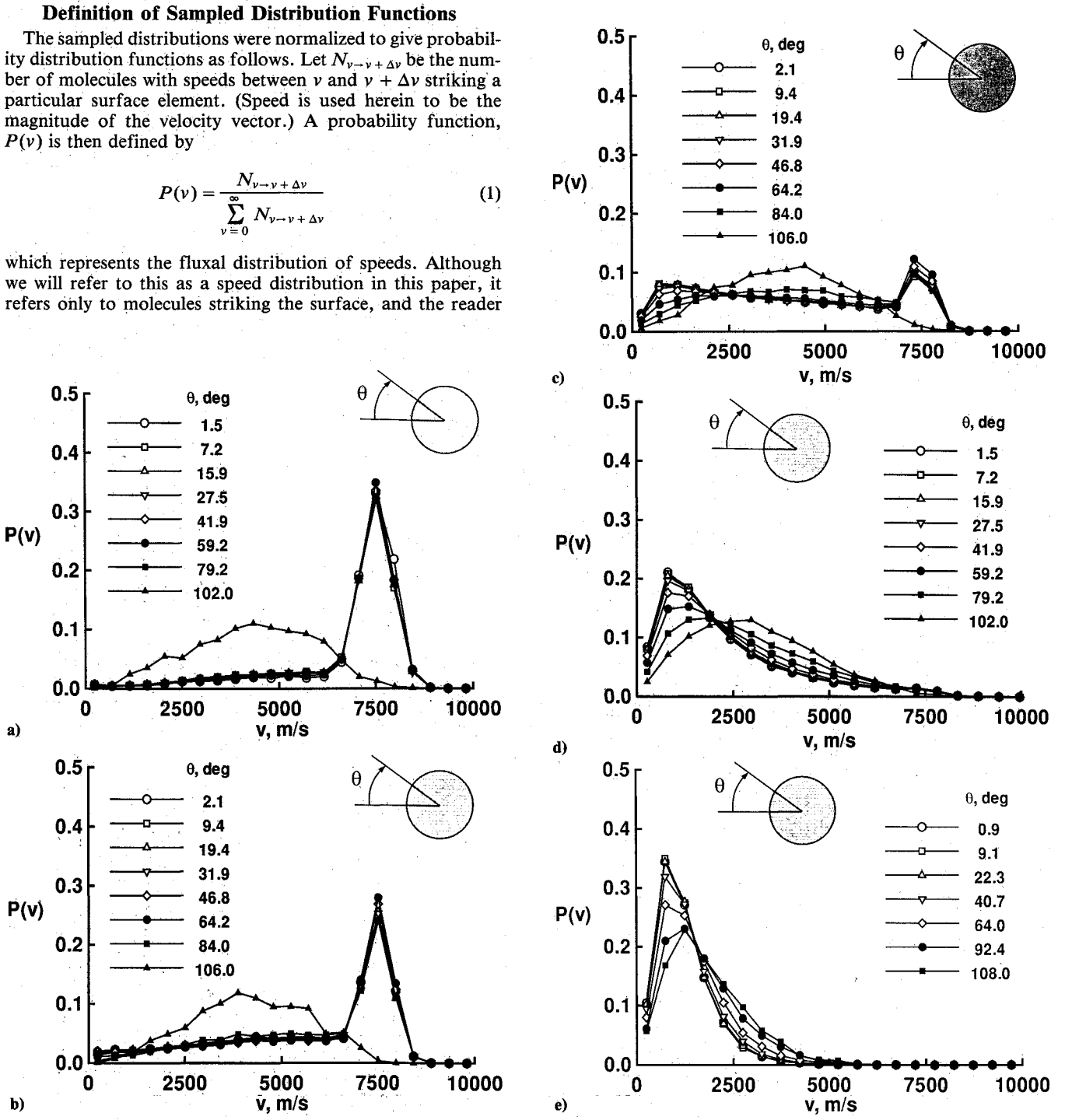

Fig. 4 Speed distributions of N_2 molecules striking various surface elements around a 1.6-m sphere: a) 130 km; b) 120 km; c) 110 km; d) 100 km; and e) 90 km.

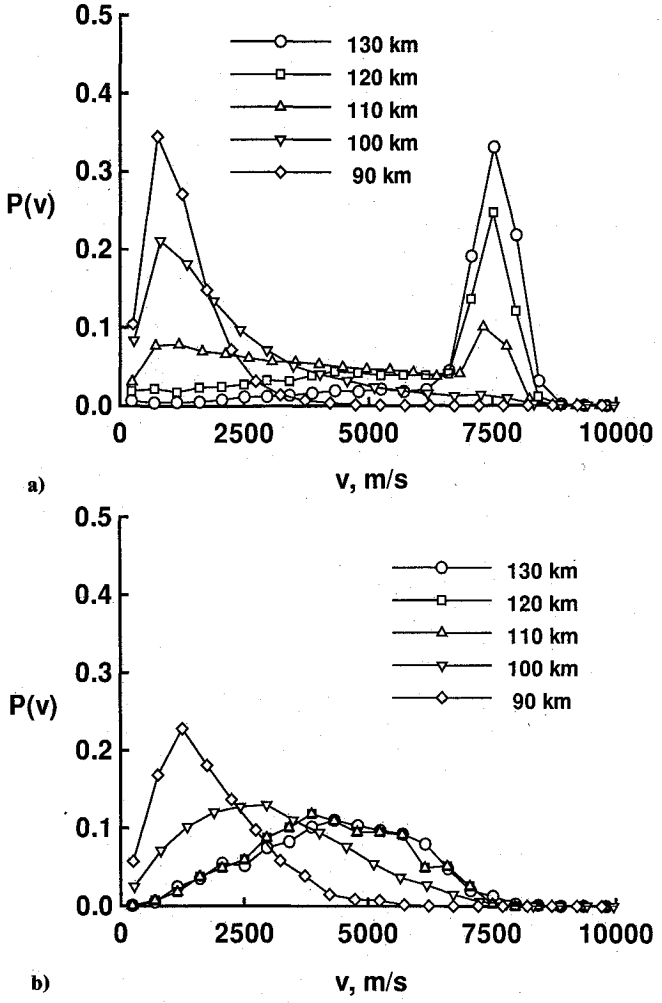

Fig. 5 Comparison of speed distributions at various altitudes (N_2 molecules): a) stagnation point; and b) leeside ($\theta \approx 105$ deg).

A cumulative energy distribution function can then be defined by

$$S^i(e_t) = \sum_{e=0}^{e_t} P^i(e) \tag{4}$$

which is the probability of having molecules of species i with energies less than or equal to e_t. (Because of the normalization used for Eq. (3), s^i can also be viewed as a cumulative probability for species i times the mole fraction of species i.) With this definition, $S_i(e_t)$ will approach a value equal to the species mole fraction of molecules striking the surface as $e_t \to \infty$.

The previous definitions are used in presenting the sampled distributions from the DSMC calculations.

Conditions of the Simulations

The flow conditions of the DSMC simulations for the 1.6-m-diam sphere at various altitudes are given in Table 1. The atmospheric conditions are those given by Jacchia[11] for an exospheric temperature of 1200 K. The surface temperature of the sphere was assumed to be constant at 350 K. The gas-surface interaction was assumed to be diffuse with full thermal accommodation, and the surface was assumed to be noncatalytic. Knudsen numbers based on sphere diameter varied from about 0.01 at 90 km altitude to about 5 at 130 km. The chemical kinetics model given by Moss[12] was used (five species, O_2, N_2, O, N, and NO, with 23 reactions).

The simulations were conducted using molecule/cell specifications ranging from about 20000 molecules and 300 cells at 130 km to about 35000 molecules and 1500 cells at 90 km. Samples were accumulated after achieving steady-state conditions over a large number of timesteps (as large as 100,000). The number of sampling timesteps was dictated by the requirement that the total sample size of particles striking the surface be at least one million molecules.

Results and Discussion

Stagnation Profiles

Profiles of the density, temperature, and species mass fraction along the stagnation line are shown in Figs. 2 and 3 for altitudes of 130 and 90 km. At 130 km, a density rise of about 22 times the freestream value occurs over a relatively large distance (≈ 3 m). However, temperatures associated with the internal modes (rotation and vibration) remain essentially constant at the freestream temperature indicating that very few collisions occur. The large increase in translational temperature in the merged shock layer near the body is caused by the

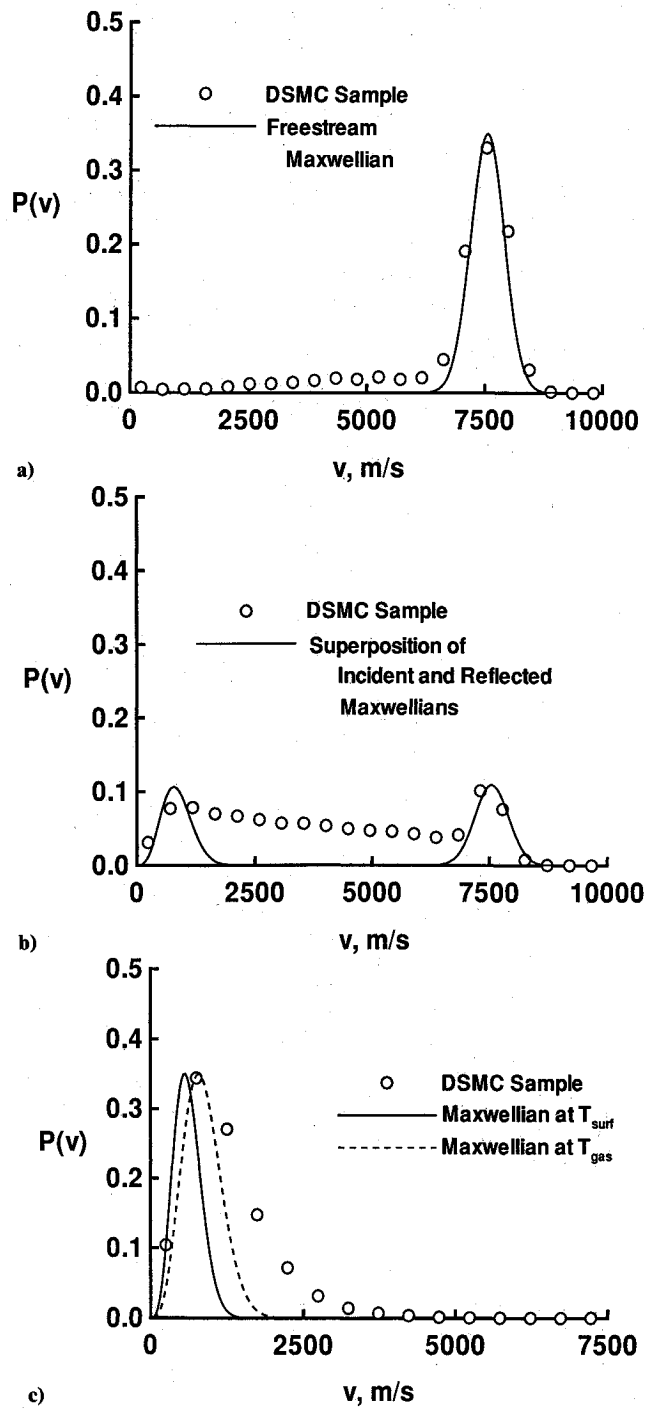

Fig. 6 Comparison of DSMC-sampled speed distributions with various Maxwellian-derived distributions (N_2 molecules at stagnation point): a) 130 km; b) 110 km; and c) 90 km.

bimodality in the velocity distribution rather than by collisions. In the free-molecular limit, it can be shown that this bimodality must occur and is just the superposition of the freestream and reflected velocity distributions.

At 90 km, the density increases to well over 100 times the freestream value over a much shorter distance (≈ 0.1 m). Collisions become very significant, and there is considerable excitation of the internal modes and considerable chemical activity (see Figs. 2b and 3b). Although there is still a high degree of thermal nonequilibrium, these conditions give a more continuum-like behavior than those at 130 km.

Speed Distributions

Speed distributions are presented in Fig. 4 for N_2 molecules striking various surface elements around the sphere and at various altitudes. Results are presented for selected surface elements as a function of the circumferential angle θ of the center of the element, where elements with $\theta > 90$ deg are on the leeside of the sphere. Since the number of elements and their angular position were not the same for all altitudes, the values of θ selected do not match exactly for all altitudes.

At the higher altitudes (130 and 120 km), the majority of molecules striking the windward side are distributed in a narrow peak around the freestream velocity (7500 m/s). There is also very little variation over the different windward surface elements. However, on the leeside, the molecules are distributed over a much broader range of speeds centered around a speed that is lower than the freestream velocity. The broadening of the distribution on the leeside results for two reasons. First, surface elements on the leeside see fewer particles traveling near or above the freestream speed than those striking the windward side because of the shielding effect of the body. In fact, in free-molecular flow, it can be shown that at the rear stagnation point, only molecules from the high-speed thermal tail of the distribution (in a reference frame moving at the freestream velocity) can reach the surface, and the resulting speed distribution (in the body frame of reference) of these molecules will be approximately that of a Maxwellian flux distribution corresponding to the freestream temperature. (Although the axial component of velocity comes from the high-speed tail, the velocity components normal to the freestream direction are still distributed according to a Maxwellian distribution.) Second, molecules can reach the leeside surface as a result of gas-gas collisions which may also lead to a broadening of the distribution. However, for the present simulations, the number of sample particles reaching surface elements near the rear stagnation point was insufficient to accurately determine the speed distribution.

At 110 km, the speed distributions show a marked difference from those at the higher altitudes. Near the stagnation point, the distribution is bimodal with the appearance of a low-speed peak (near 1000 m/s) and a marked decrease in the amplitude of the high-speed peak corresponding to freestream molecules. The distributions also show more variation around the circumference of the sphere and, on the leeside, are similar to those at the higher altitudes. At the lower altitudes of 100 and 90 km, the freestream peak essentially disappears indicating that a negligible fraction of the molecules reach the surface without undergoing one or more collisions.

The variations with altitude are summarized in Fig. 5 for a surface element near the stagnation point and an element on the leeside of the sphere. On the stagnation point, the distributions transition from that for a nearly collisionless flow at 130 km to that for a collision-dominated flow at 90 km. For the leeside element, the distributions are essentially the same at 110 km and above, but at 90 and 100 km, they show a more continuous transition from the windward side to the leeward side than at higher altitudes. This indicates that the density is high enough at the lower altitudes to give a more continuum-like turning of the flow around the sphere.

Table 1 Freestream conditions

Altitude, km	ρ_∞, kg/m^3	v_∞, km/s	T_∞, K	Mole fraction O_2	Mole fraction N_2	Mole fraction O	$\bar{M}$, g/mol	λ_∞, m
90	3.43×10^{-6}	7.5	188	0.209	0.788	0.004	28.80	0.017
100	5.66×10^{-7}	7.5	194	0.177	0.784	0.040	28.24	0.100
110	9.67×10^{-8}	7.5	247	0.123	0.770	0.106	27.22	0.599
120	2.27×10^{-8}	7.5	368	0.085	0.733	0.183	26.14	2.681
130	8.23×10^{-9}	7.5	500	0.071	0.691	0.238	25.43	7.724

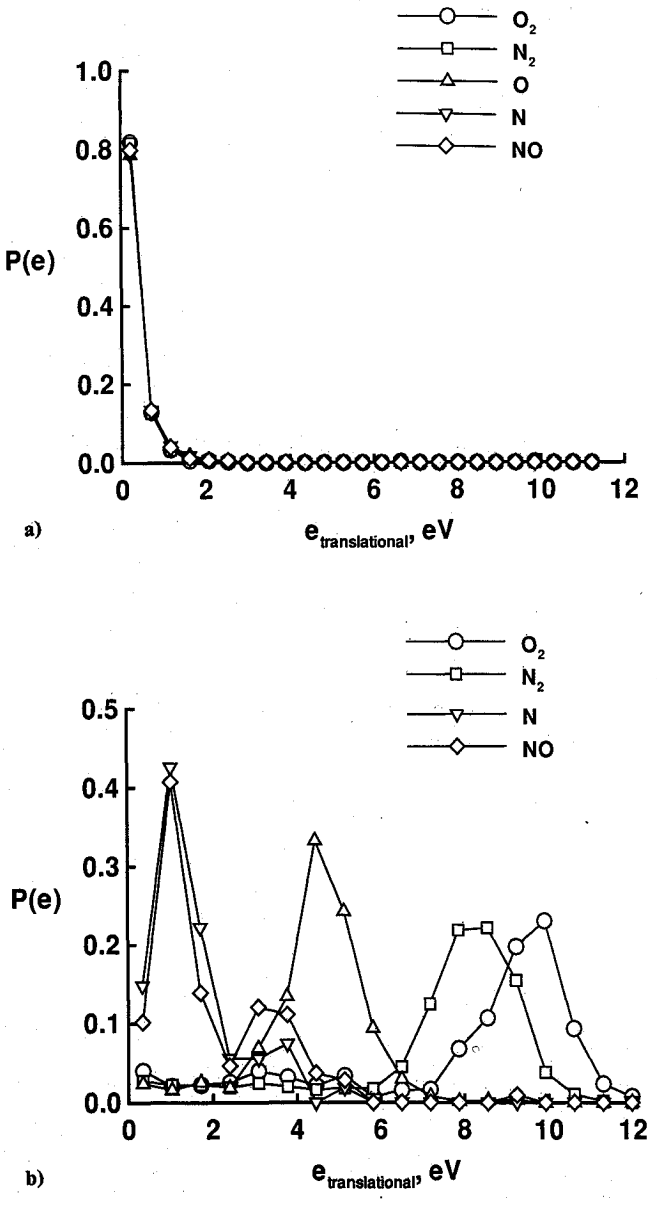

Fig. 7 Translational energy distributions for various species (stagnation point): a) 130 km; and b) 90 km.

The speed distributions sampled for molecular and atomic oxygen (O_2 and O) showed a behavior similar to that for molecular nitrogen. However, the species N and NO, which are not present in the freestream gas, seemed to have a much different behavior. Unfortunately, for the present calculations, these species were not produced in sufficient quantities to allow accurate sampling of the distributions. Some limited information is given in a later section on these species.

Comparisons with Maxwellian Distributions

A partial explanation for the behavior shown in the speed distributions can be seen in Fig. 6 by the comparisons of the DSMC results at the stagnation point with various distribu-

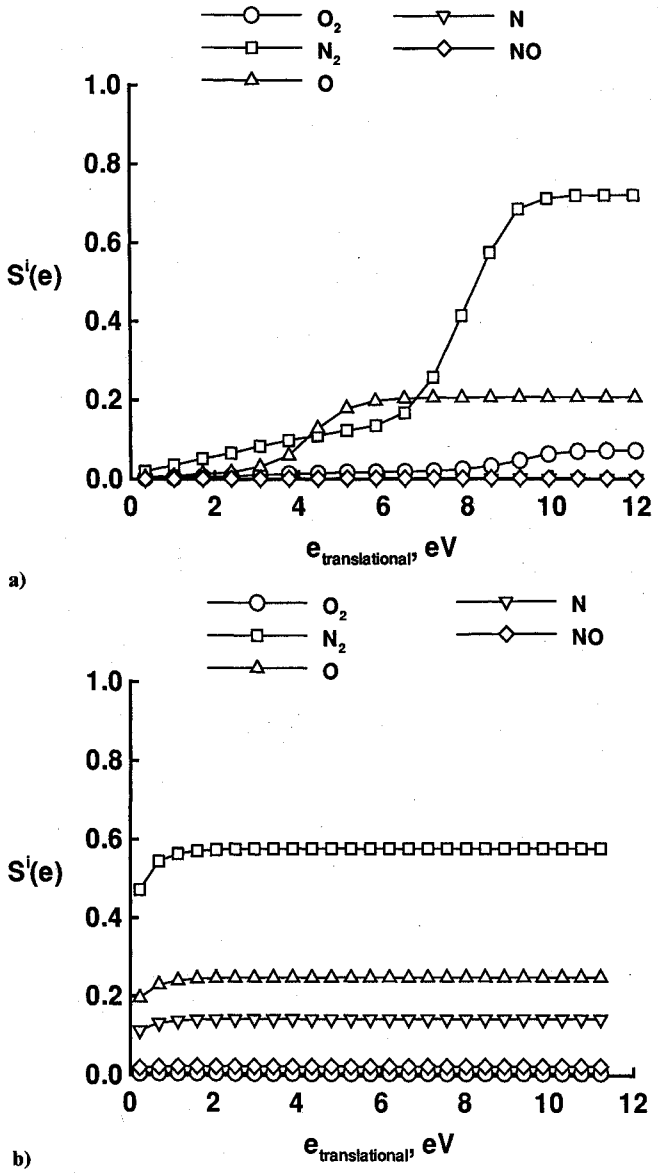

Fig. 8 Translational energy cumulative probability distributions for various species (stagnation point): a) 130 km; and b) 90 km.

tions derived from an equilibrium Maxwellian distribution. At 130 km (see Fig. 6a), the flow is approximately free molecular, and the incident flux distribution in speeds for particles striking the windward surface at the stagnation point can be approximated by a distribution of the form

$$P_\infty(v) \propto v^3 e^{-\beta^2(v-v_\infty)^2} \tag{5}$$

where v is the molecular speed, $\beta^2 = m/2kT_\infty$, m is the molecular mass, k is Boltzmann's constant, T_∞ is the temperature in the undisturbed freestream, and v_∞ is the mean freestream speed. This distribution corresponds approximately to that for a Maxwellian distribution of thermal velocities superimposed on the freestream velocity and is sufficiently accurate for the hypersonic conditions of the present simulation. (The exact form of the freestream velocity distribution for a streaming Maxwellian written in the body frame of reference is a function of the angle of incidence of molecules to the surface element. However, using the cylindrical symmetry at the stagnation point and integrating over all incidence angles, it can be shown that the form given by Eq. (5) is a reasonable representation of the speed flux distribution.) At 130 km, the DSMC results show reasonably good agreement with this distribution, although there is a slight excess of lower speed molecules due to the few gas-phase collisions that do take place.

At 90 km (see Fig. 6c), a comparison is made with flux distributions arising when the incident gas molecules can be described by an equilibrium Maxwellian distribution, and distributions are given for two different temperatures: one corresponding to the surface temperature and the other corresponding to a temperature associated with the gas in the DSMC computational cell adjacent to the surface. (Although the gas adjacent to the surface may not be in thermal equilibrium, a temperature can be defined from the DSMC results using $3/2(kT_{gas} = 1/2m(\overline{v^2} - \overline{v}^2)$ such that a Maxwellian distribution at T_{gas} should match the DSMC result as the flow approaches equilibrium. The Maxwellian distribution has a form similar to Eq. (5) as $v_\infty \to 0$ and T_∞ is replaced with T_{gas}.) Although the Maxwellian distribution corresponding to T_{gas} matches the DSMC result better than the Maxwellian at T_{surf}, there is a definite excess in higher speed molecules in the DSMC result.

At the intermediate altitude of 110 km, one might expect the distribution to be approximated by a superposition of the freestream distribution (streaming Maxwellian) and an equilibrium Maxwellian corresponding to the temperature T_{gas}. A comparison of such a superposition with the DSMC result (see Fig. 6b) shows that the bimodal peaks are located at about the same speeds as the Maxwellian-derived distribution. (The relative magnitudes of the two peaks in the Maxwellian superposition was arbitrarily selected to be equal.) However, the DSMC result shows a broad distribution of molecules at speeds between the two peaks that is definitely non-Maxwellian. Although such a behavior might be qualitatively expected since intermolecular collisions are becoming significant, the exact origin of this non-Maxwellian behavior was not determined in the present study. Further DSMC calculations in which the collision history of the molecules is recorded would be useful in determining the origin of molecules that appear at these intermediate speeds.

Energy Distributions

Translational energy distributions are given in Fig. 7 for each of the five species at altitudes of 130 and 90 km. Although the translational energy can be derived from the speed distribution, it is useful to note that the energy distribution form allows one to more readily discriminate molecules (or atoms) of different masses. For the freestream species (O_2,

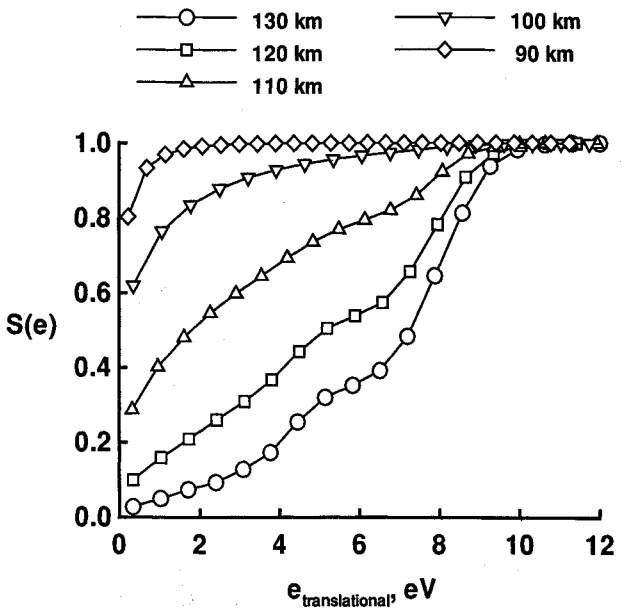

Fig. 9 Cumulative translational energy distributions summed over all species (stagnation point).

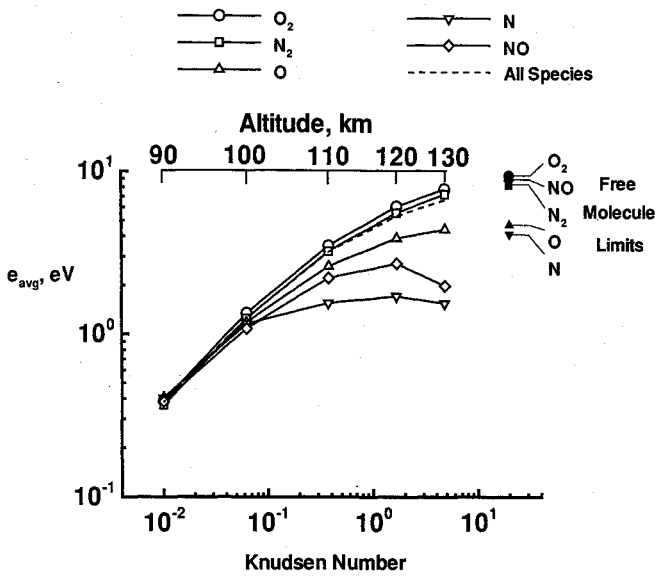

Fig. 10 Average translational energy per particle striking the surface at the stagnation point. (Free-molecule limits for freestream particles shown as filled symbols.)

N_2, and O) at 130 km, the peaks in the energy distribution are indeed spaced in proportion to the species molecular weights. However, for the species N and NO (produced by dissociation and chemical reaction), the peak in the energy distribution occurs at a much lower energy than that at which it would occur if these species were present in the freestream gas. (Because of the small sample size for these species, one should not attempt to draw conclusions about the detailed shape of the distributions for N and NO.) At 90 km, the size of the DSMC sampling "bins" is too large to resolve the details of the energy distribution, and the results for all species appear to collapse to the same curve.

Cumulative distributions defined by Eqs. (3) and (4) are shown in Fig. 8. Since the cumulative distribution approaches the mole fraction of each species at large energies, it can be seen that at 130 km, over 70% of the particles that reach the surface are N_2, 20% are O, and less than 10% are O_2 with negligible amounts of N and NO. At 90 km, the approximate percentages are 58, 25, 14, and 3% for N_2, O, N, and NO, respectively, with only a trace amount of O_2.

Cumulative distributions obtained by summing over all species are shown in Fig. 9 for each altitude. It is observed that at 130 km, over 95% of all molecules have energies greater than 1 eV, while at 90 km, over 90% have energies less than 1 eV. Because of the unknown sensitivity of gas-surface interactions to the incident energy of the gas molecules, it might be speculated that the range of altitudes studied here could produce significant variations in the type of interaction (e.g., diffuse vs specular, amount of momentum and energy accommodation). Of course, implicit in the present calculations is the assumption of diffuse scattering with complete accommodation. It will be necessary to do further calculations to determine the sensitivity of the results to the gas-surface scattering model.

Need for Experiments

The average energy per particle for molecules striking the surface is given in Fig. 10 as a function of Knudsen number and altitude. The average energy varies from <0.4 eV at a Knudsen number of 0.01 to almost 10 eV at a Knudsen number of 5 and approaches the free-molecular limit for a velocity of 7.5 km/s at the higher Knudsen number.

With such a wide variation in gas-surface interaction energies in this transitional regime, there is a strong need for experiments that can illuminate the nature of the interactions over this energy range. Flight experiments such as those proposed by Hurlbut[10] or variations on those performed by Gregory and Peters[13] might be useful for the high-energy range. There is also a considerable amount of experimental data available at very low thermal energies (<0.05 eV). However, to provide a smooth transition in DSMC modeling capability for entry flows ranging from near-continuum to free-molecule, a significant effort is needed to "fill in the gap" between low- and high-energy gas-surface interactions. The importance of surface and material characterization in such experiments cannot be overemphasized.

Concluding Remarks

The DSMC method has been used to study the speed and energy distributions of molecules reaching the surface after traversing a shock layer in hypersonic transitional flow. The results show that there are significant variations in the speed and energy of molecules reaching the surface over an altitude range of 130–90 km. Speed distributions vary from those expected for hypersonic, free-molecular flow at high altitudes (large Knudsen numbers) to those expected for near-equilibrium continuum-like flows at low altitudes (low Knudsen numbers). At intermediate altitudes, the distributions are bimodal with a broad range of speeds resulting from gas-gas collisions. Although the bimodality can be described simply by a superposition of Maxwellian-like distributions, the broadening of the distribution is definitely non-Maxwellian.

The mean energies of the molecules reaching the surface varied from about 0.4 eV at a Knudsen number of 0.01 to almost 10 eV at a Knudsen number of 5. Since the results of the DSMC simulations depend on the assumptions about the gas-surface interaction, further study is needed to determine the sensitivity of the results to the model parameters. Because of the wide range in energy for incident molecules, there is also a need for experiments to measure the sensitivity of the model parameters to the incident energy and incidence angle for various gas-surface combinations. The results of the study are intended to provide information that will be useful to those designing such experiments for transitional flows at entry velocities.

Acknowledgments

The authors wish to express their appreciation to Didier Rault and Graeme Bird for many helpful discussions.

References

[1]Hurlbut, F. C., "Particle Surface Interaction in the Orbital Context: A Survey," *Rarefied Gas Dynamics,* edited by E. P. Muntz, D. P. Weaver, and D. H. Campbell, Vol. 116, Progress in Astronautics and Aeronautics, AIAA, New York, 1989, pp. 419–450.

[2]Muntz, E. P., "Rarefied Gas Dynamics," *Annual Review of Fluid Mechanics,* Vol. 21, 1989, pp. 387–417.

[3]Bird, G. A., "Monte-Carlo Simulation in an Engineering Context," *Rarefied Gas Dynamics,* edited by S. S. Fisher, Vol. 74, Pt. 1, Progress in Astronautics and Aeronautics, AIAA, New York, 1981, pp. 239–255.

[4]Moss, J. N., and Bird, G. A., "Monte Carlo Simulations in Support of the Shuttle Upper Atmospheric Mass Spectrometer Experiment," AIAA Paper 85-0968, June 1985.

[5]Dogra, V. K., and Moss, J. N., "Hypersonic Rarefied Flow About Plates at Incidence," AIAA Paper 89-1712, June 1989.

[6]Bartel, T. J., and Hudson, M. L., "Energy Accommodation Modeling of Rarefied Flow Over Re-Entry Geometries Using DSMC," AIAA Paper 89-1879, June 1989.

[7]Caledonia, G. E., "Laboratory Simulations of Energetic Atom Interactions Occurring in Low Earth Orbit," *Rarefied Gas Dynamics,* edited by E. P. Muntz, D. P. Weaver, and D. H. Campbell, Vol. 116, Progress in Astronautics and Aeronautics, AIAA, New York, 1989, pp. 129–142.

[8]Dogra, V. K., Wilmoth, R. G., and Moss, J. N., "Aerothermodynamics of a 1.6-m-Diameter Sphere in Hypersonic Rarefied Flow," AIAA Paper 91-0772, Jan. 1991

[9]Wood, G. M., Wilmoth, R. G., Carlomagno, G. M., and deLuca, L., "Proposed Aerothermodynamic Experiments in Transition Flow

Using the NASA/ASI Tethered Satellite System-2," AIAA Paper 90-0536, Jan. 1990.

[10]Hurlbut, F. C., and Potter, J., "Tethered Aerothermodynamic Research Needs," AIAA Paper 90-0553, Jan. 1990.

[11]Jacchia, L. G., "Thermospheric Temperature, Density, and Composition: New Models," Smithsonian Astrophysical Observatory Special Rept. 375, Cambridge, MA, March 15, 1977.

[12]Moss, J. N., and Bird, G. A., "Simulation of Transitional Flow for Hypersonic Re-Entry Conditions," *Thermal Design of Aeroassisted Orbital Transfer Vehicles,* edited by H. F. Nelson, Vol. 96, Progress in Astronautics and Aeronautics, AIAA, New York, 1985, pp. 113–139.

[13]Gregory, S. J., and Peters, R. N., "A Measurement of the Angular Distribution of 5 eV Atomic Oxygen Scattered off a Solid Surface in Earth Orbit," *Rarefied Gas Dynamics,* edited by V. Boffi and C. Cercignani, Vol. I, B. G. Teubner, Stuttgart, Germany, 1986, pp. 644–656.

Gerald T. Chrusciel
Associate Editor